

**Advanced Microwave Guided-Structures and Analysis**  
**Professor Batin Ghosh**  
**Indian Institute of Technology, Kharagpur**  
**Department of Electronics & Electrical Communication Engineering**  
**Lecture 67**

**Application to the Coupling Problem: Aperture-Coupled, Probe-Coupled and Waveguide Coupled Structures (Contd.)**

So, welcome to the continuation of the lecture on the application of the concepts learned on the Aperture Coupled and Probe Coupled and the Waveguide Coupled Structures. The topic which we were on was the difference between the source free and the loaded resonance.

(Refer Slide Time: 00:37)

- First resonance dip at 3.08 GHz is close to the source free resonant frequency of  $TE_{111}$  mode at 3.18 GHz.
- Second resonance dip at 3.42 GHz is stub resonance.
- Calculated 10 dB impedance bandwidth is 26.80%.
- Measured 10 dB impedance bandwidth is 29.17%.
- Antenna is easier to fabricate due to the air used in the second DRA layer.

6

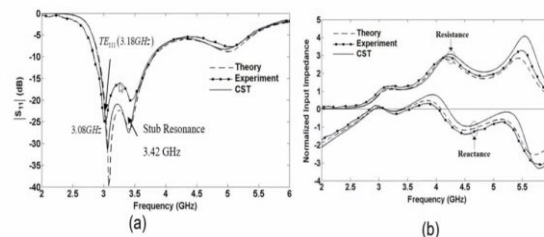


Fig. 1: Calculated, simulated and measured return loss and normalized input impedance of the microstrip slot-coupled three-layer DRA with centred slot excited in the  $TE_{111}$  mode :  $\epsilon_{r1} = 9, \epsilon_{r2} = 1, \epsilon_{r3} = 4, r_1 = 12.5mm, r_2 = 17.5mm, r_3 = 22.5mm, L_1 = 14.5mm, W_1 = 1.0mm, x_c = 0mm, y_c = 0mm, \sigma_{r1} = 2.2, h = 0.508mm, W_f = 1.58mm, L_{ob} = 6.25mm, \Delta l = 0.25mm$  (a) Return loss. (b) Normalized input impedance.

So, as we were seeing last time that the first resonant dip in this figure was at 3.08 gigahertz contributed by the  $TE_{111}$  mode. We now understand, what is the  $TE_{111}$  mode in terms of this

modal indices, and the second resonance by the stub resonance. Now we see that the first resonant dip is close to the source free resonant frequency of the  $TE_{111}$  mode.

So, it is seen that the first resonance is close to the source free resonance of the  $TE_{111}$  mode. Now what is the difference between 3.08 and 3.18, why are they different. So, one is the loaded resonance. And the other is known as the source free resonance.

(Refer Slide Time: 01:38)

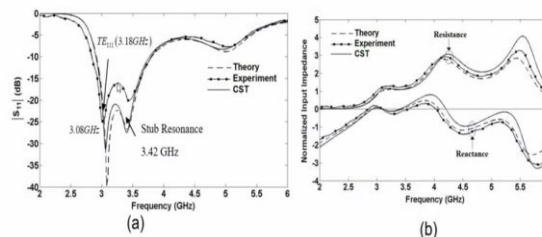
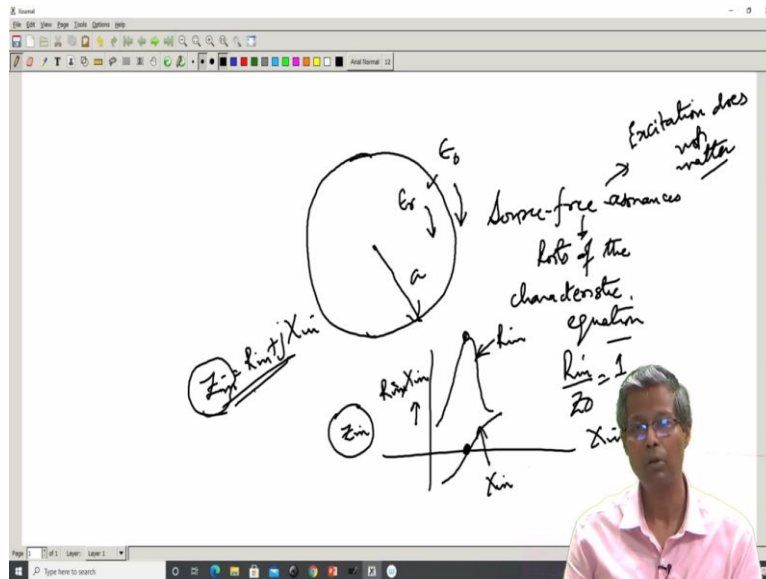


Fig 1: Calculated, simulated and measured return loss and normalized input impedance of the microstrip slot-coupled three-layer DRA with centred slot excited in the  $TE_{111}$  mode:  $\epsilon_{r1}=9$ ,  $\epsilon_{r2}=1$ ,  $\epsilon_{r3}=4$ ,  $r_1=12.5\text{mm}$ ,  $r_2=17.5\text{mm}$ ,  $r_3=22.5\text{mm}$ ,  $L_z=14.5\text{mm}$ ,  $W_s=1.0\text{mm}$ ,  $x_0=0\text{mm}$ ,  $y_0=0\text{mm}$ ,  $\epsilon_{r2}=2.2$ ,  $h=0.508\text{mm}$ ,  $W_f=1.58\text{mm}$ ,  $L_{ob}=6.25\text{mm}$ ,  $\Delta l=0.25\text{mm}$ . (a) Return loss. (b) Normalized input impedance.

- First resonance dip at 3.08 GHz is close to the source free resonant frequency of  $TE_{111}$  mode at 3.18 GHz.
- Second resonance dip at 3.42 GHz is stub resonance.
- Calculated 10 dB impedance bandwidth is 26.80%.
- Measured 10 dB impedance bandwidth is 29.17%.
- Antenna is easier to fabricate due to the air used in the second DRA layer.

6

To differentiate between the two, let us see that if I have the resonator like the one shown in above fig. As we said, the resonant frequencies come by matching the electric and magnetic fields at this interface. The radius of the resonator is 'a'. So, by matching the electromagnetic fields, the tangential electric and magnetic fields at this interface yields to the characteristic equation and the roots of the characteristic equation correspond to the source free resonance. So, the source free resonances are nothing but the roots of the characteristic equation.

The loaded resonance, on the other hand, is the resonance, at which the analytical tool or the simulation engine gives me zero crossing of the input reactance. So, let us see here with respect to the figure. So, this zero crossing of the input reactance near 3 gigahertz. So, this zero crossing and the normalized resistance, which is  $R_{in} / Z_0$ , close to 1. So, the input resistance is close to 50 ohm and the input reactance is close to 0. What does that mean?

Let us go to the figure again. So, let us say, if my input resistance is close to 50, I will get a match. So,  $R_{in} / Z_0$  will be close to 1 and  $X_{in}$  will be close to 0. So, this corresponds to the loaded resonance.

So, what is the loaded resonance? How is it physically different from the source free resonance? The loaded resonance takes into account, the presence of the excitation source, in this case the presence of the slot. The source free resonance has nothing to do with the excitation. It has nothing to do with the excitation. Excitation does not matter. It has nothing to do with the excitation, while the loaded resonance is then accurate analysis of the circuit or the antenna structure. It takes into account the excitation and everything is taken into account to find the actual input impedance.

So,  $Z_{in}$  which is equal to  $R_{in} + j X_{in}$ . So, it evaluates  $Z$  in taking into account the presence of the excitation source and that is called the loaded resonance. So, we see that the loaded resonance is as important, or I should say, the source free resonance is as important as the loaded resonance, because the source free resonance gives me the information as to which mode is close to the  $S_{11}$  dip.

So, the dip in  $S_{11}$  corresponding to the matching condition, which mode is principally contributing to that resonance. This information is provided by the source free resonance that is why we search the source free resonances near a particular loaded resonance. So, let us go back to the presentation.

So you see now, so the first resonance which is the loaded resonance is a 3.08 gigahertz and the source free resonance of the  $TE_{111}$  mode is 3.18 gigahertz. So, it is contributed by the source free  $TE_{111}$  mode. The second resonance dip is at 3.42 gigahertz is the stub resonance. So, this is the stub resonance. Now the calculated 10 dB bandwidth is 26.8 percent and the measured 10 dB bandwidth was 29.17 percent.

The calculation was done using the full wave Green's function technique as we said before. But we are not going to concern ourselves with that. But that is intimately dependent or as a direct result of the modal concepts, which we learned for the waveguide structures. So, the Green's function technique relies heavily on or it is an expression of the origin or an extension of the modal concepts or the concept behind the, or the theory of the modes. So, essentially, it is also called the scalar Green's function technique, which we used here.

And in which the fields are expressed as a summation over the modal indices, just like the fields of the rectangular waveguide or the fields of the cylindrical structure, which we consider that they are a summation over the modal indices. So, just like that we have considered the summation over the modal indices and we found the amplitude of the individual modes and that is how we calculate the total field or the total greens function and that is the calculated 10 dB impedance bandwidth.

The measured impedance bandwidth is 29.17. And particularly this antenna is easier to fabricate. Why do we say that it is easier to fabricate? Because of the presence of air, in the middle layer. And there might be, you know like, the mechanical problem of gluing, the problem of air gaps and things like that, which are avoided by choosing the middle layer

dielectric constant to be 1. So, next, so we see that the total bandwidth is 30, about 30 percent, using this kind of a structure.

(Refer Slide Time: 09:05)

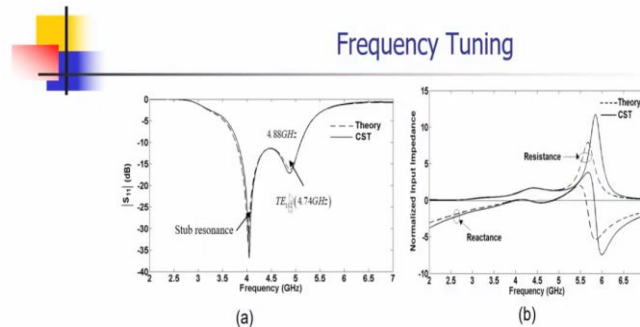


Fig. 2 : Calculated and simulated return loss and normalized input impedance of the microstrip slot-coupled three-layer DRA with centred slot excited in the  $TE_{112}$  mode :  $r_1 = 18.5mm$ ,  $r_2 = 23.5mm$ ,  $L_1 = 12.0mm$ ,  $L_{stub} = 4.45mm$ . The other parameters are the same as in Fig. 1. (a) Return loss. (b) Normalized input impedance.



So, the next is we demonstrate the frequency tuning of this structure. Now when we shift the frequency, we essentially excite a higher order mode, in this case the  $TE_{112}$  mode. So, you see here that the third model in this index p which is 2 that is changed resulting in a change of the resonant frequency without a change in the field distribution.

Because the field distribution are contributed by n and m, which is 1 and 1 here, which are unaffected, which are unaltered, therefore the field distribution of the  $TE_{112}$  mode is exactly going to be the same as the  $TE_{111}$  mode, which we discussed in the previous example.

So, this is also the case of the centered slot with  $r_2$  equal to 18.5 millimeter,  $r_3$  as 23.5 millimeter, the length of the slot l is 12 millimeter and the length of the stub 4.45 millimeter and all the parameters are the same as in the previous case. And this shows that the two resonances, the first resonance is the stub resonance and the second resonance is contributed by the  $TE_{112}$  mode.

(Refer Slide Time: 10:16)



- First resonance dip at 4.02 GHz is stub resonance.
- Second resonance dip at 4.88 GHz is close to the source free resonant frequency of  $TE_{112}$  mode at 4.74 GHz.
- Calculated 10 dB impedance bandwidth is 30.18%.
- The center frequency for the return loss bandwidth in Fig. 2(a) is at 4.44 GHz which is displaced from the center frequency of 3.36 GHz in Fig. 1(a) by 32.14 %.

8



- First resonance dip at 3.08 GHz is close to the source free resonant frequency of  $TE_{111}$  mode at 3.18 GHz.
- Second resonance dip at 3.42 GHz is stub resonance.
- Calculated 10 dB impedance bandwidth is 26.80%.
- Measured 10 dB impedance bandwidth is 29.17%.
- Antenna is easier to fabricate due to the air used in the second DRA layer.

6



## Frequency Tuning

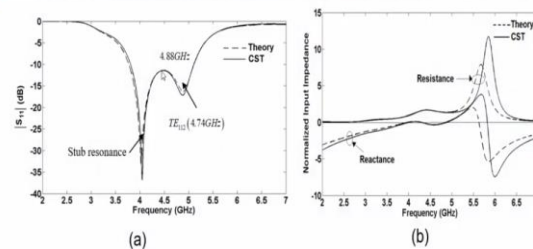


Fig. 2 : Calculated and simulated return loss and normalized input impedance of the microstrip slot-coupled three-layer DRA with centred slot excited in the  $TE_{112}$  mode :  $r_1 = 18.5mm$ ,  $r_2 = 23.5mm$ ,  $L_1 = 12.0mm$ ,  $L_{20} = 4.45mm$ . The other parameters are the same as in Fig. 1. (a) Return loss. (b) Normalized input impedance.



7

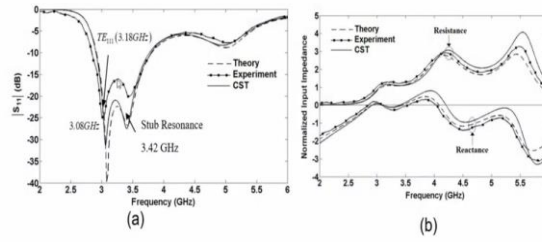


Fig. 1: Calculated, simulated and measured return loss and normalized input impedance of the microstrip slot-coupled three-layer DRA with centred slot excited in the  $TE_{111}$  mode :  $\epsilon_{r1} = 9$ ,  $\epsilon_{r2} = 1$ ,  $\epsilon_{r3} = 4$ ,  $r_1 = 12.5mm$ ,  $r_2 = 17.5mm$ ,  $r_3 = 22.5mm$ ,  $L_z = 14.5mm$ ,  $W_z = 1.0mm$ ,  $x_0 = 0mm$ ,  $y_0 = 0mm$ ,  $\epsilon_{r2} = 2.2$ ,  $h = 0.508mm$ ,  $W_f = 1.58mm$ ,  $L_{ob} = 6.25mm$ ,  $\Delta l = 0.25mm$ . (a) Return loss. (b) Normalized input impedance.



So, the first dip is at 4.02 gigahertz, is a stub resonance and the second resonance at 4.88 gigahertz, is close to the source free resonance of the  $TE_{112}$  mode, which has a source free resonance of 4.74 gigahertz. And as a result the calculated 10 dB impedance bandwidth is 30.18 percent, which is kind of the same as we obtained before. So, we demonstrate the frequency tuning of this antenna.

So we see that the center frequency for the return loss bandwidth in figure 2 a, is at 4.44 gigahertz. So, you see this is at 4.44 gigahertz, close to 4.5, and which is displaced from the center frequency of 3.36 gigahertz in figure 1 a.

So, in figure 1 a, so center resonance frequency is 3.36 gigahertz and the displacement is by 32.14 percent. So, we shifted the resonance frequency without any effect on the radiation characteristics or the bandwidth. It is still the same broadband structure and we get the same radiation characteristics as we obtained before for the figure 1.

(Refer Slide Time: 11:51)

### Slot offset along slot length

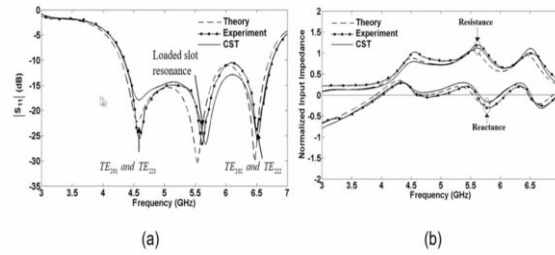


Fig. 3 : Calculated, simulated and measured return loss and normalized input impedance of the microstrip slot-coupled three-layer DRA for y-offset slot :  $r_1 = 16.5mm$ ,  $r_2 = 22.0mm$ ,  $L_2 = 12.0mm$ ,  $L_{20} = 7.75mm$ ,  $y_w = 4mm$ . The other parameters are the same as in Fig.1 . (a) Return loss. (b) Normalized input impedance.

Next, we investigate the case of a slot offset along slot length. So, here, we see that we get three resonant dips. The first resonant dip is contributed by the  $TE_{201}$  and  $TE_{221}$  mode together. So, these are degenerate modes. So, they have the same resonance frequency. So, you see that the n and p, the first and the third modal index, are the same for these two modes, so they will have the same resonant frequencies, because n and p are the same.

However, the second index, which is contributing to the field distribution, is different. So, that means we have to investigate that how the field of  $TE_{201}$ , how much it is different from  $TE_{221}$ . If it is too much different, it is cause for concern, we should be aware of this fact. Because there is a presence of two degenerate modes, having the same resonant frequencies. But having two different field distributions, contributed by the difference in the second modal index.

The same happens at the third resonant frequency, at the third, at the third dip of  $S_{11}$ . We have the third dip, which is contributed essentially by the third modal index here, it is 1 here, here, it is 2 here. And these two again are degenerate  $TE_{202}$  and  $TE_{222}$ , because n and p are the same here.

So therefore, we have to see, exactly how much the  $TE_{202}$  and how much the  $TE_{222}$ , how much they are excited, to the extent they are excited? And whether they interfere with each other's pattern? So, we have to be concerned about that. So, you see how the knowledge of the modes enables us, to focus on regions, which might lead to the concept of like the polarization purity of the modes.

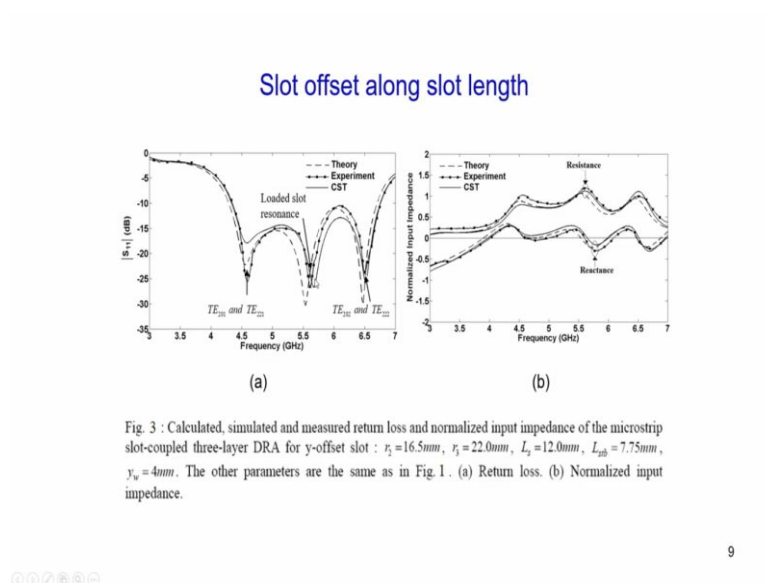
That is the extent to which the radiation characteristics of 1 mode is affected by or may be affected by the presence of another degenerate mode.

So, this is where the analysis comes in very handy and very very useful. The middle resonance you see is the loaded slot resonance. The loaded slot resonance means it is the slot resonance affected by the presence of the DRA. So, in this case, the y offset is given

(Refer Slide Time: 15:41)

- First resonance dip at 4.56 GHz is close to the source free resonant frequency of  $TE_{201}$  and  $TE_{221}$  modes at 4.63 GHz.
- Second resonance dip at 5.54 GHz is near the loaded slot resonance at 5.28 GHz.
- The third resonant dip in the return loss characteristics at 6.48 GHz in Fig. 3(a) is close to the degenerate  $TE_{202}$  and  $TE_{222}$  mode resonances of the three-layer HDRA at 6.26 GHz.
- Measured 10 dB impedance bandwidth is 43.42%.

10

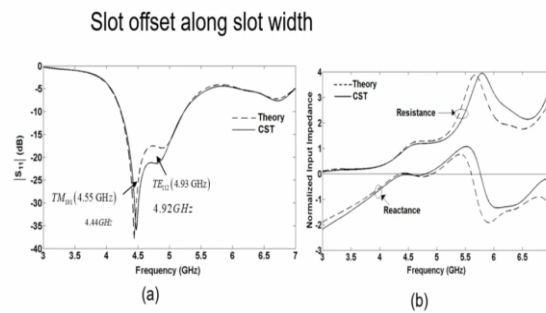


So, as we discussed, the first resonance dip at 4.56 gigahertz, here, 4.56 gigahertz here, it is close to the source free resonant frequency of the  $TE_{201}$  and  $TE_{221}$  modes at 4.63 gigahertz. The second resonance dip at 5.54 gigahertz, which is here, is near the loaded slot resonance at 5.28 gigahertz. The third resonant dip in the return loss characteristics has 6.48 gigahertz,

which is here, is close to the degenerate  $TE_{202}$  and  $TE_{222}$  mode resonances of the DRA at 6.26 gigahertz.

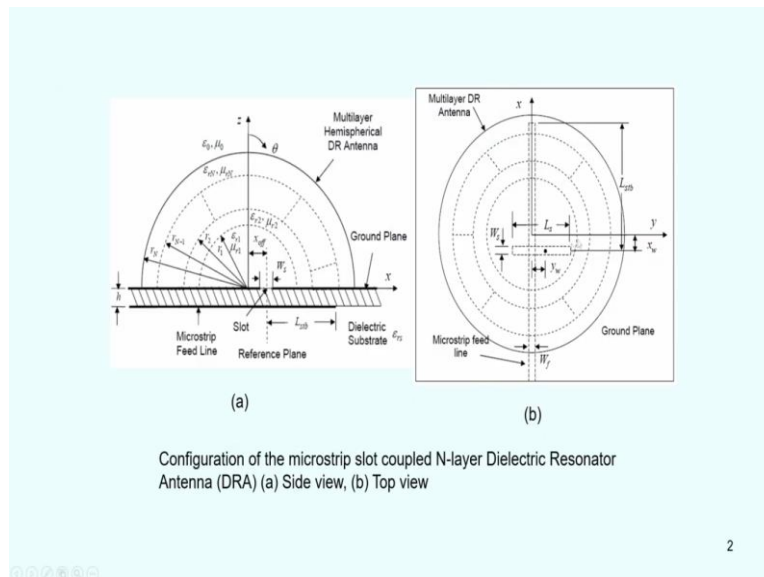
And the measured 10 dB impedance bandwidth is 43.42 percent, which is larger than our case of the centered slot. So, we see that the case of the y offset slot leads to an enhancement of a larger enhancement in bandwidth. But we have to be careful of these pattern characteristics, which might be affected by the mode degeneracy at the first and third resonances.

(Refer Slide Time: 16:52)



Calculated and simulated return loss and normalized input impedance of the microstrip slot-coupled three-layer DRA for x-offset slot :  $L_2 = 10.5mm$  ,  $L_{stub} = 3.85mm$  ,  $x_w = 4mm$  . The other parameters are the same as in Fig. 1. (a) Return loss. (b) Normalized input impedance.

11



Configuration of the microstrip slot coupled N-layer Dielectric Resonator Antenna (DRA) (a) Side view, (b) Top view

2



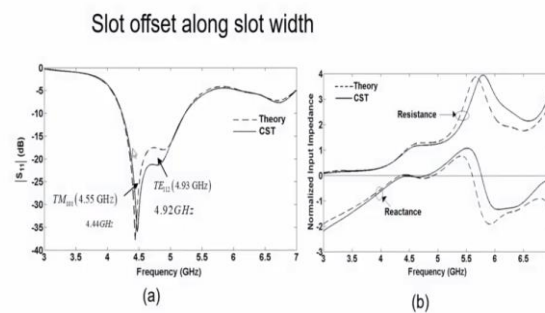
Then we do a slot offset along slot width, which is the slot offset along the X direction. The slot is offset along the X direction. So, you look at the original figure, the slot is offset along the X direction. So, when we do that we see that the first mode is excited is the  $TM_{101}$  mode. It is a TM mode and that leads to the resonance at around 4.5 gigahertz.

And the second resonance is contributed by the TE mode it is a 112 mode. It is a broad side mode with a pattern which is maximum at theta equal to 0. And it is an end fire mode in which the pattern is null, we have a null at theta equal to 0. It is an end fire pattern. So, it radiates along the horizon. So, in this case the length of the slot is 10.5 millimeter, the length of the stub is 3.85 millimeter.

(Refer Slide Time: 18:01)

- The first resonant dip at 4.44 GHz is caused due to the excitation of the  $TM_{101}$  mode with a source-free resonance frequency of 4.55 GHz.
- The second return loss dip at 4.92 GHz corresponds to the loaded resonance of the  $TE_{112}$  mode with a corresponding source-free resonance at 4.93 GHz.
- Computed 10 dB impedance bandwidth is at 21.52 %.

12



Calculated and simulated return loss and normalized input impedance of the microstrip slot-coupled three-layer DRA for x-offset slot:  $L_x = 10.5\text{mm}$ ,  $L_{z0} = 3.85\text{mm}$ ,  $x_0 = 4\text{mm}$ . The other parameters are the same as in Fig. 1. (a) Return loss. (b) Normalized input impedance.

11

So, we see that the first resonance dip at 4.44 gigahertz is caused due to the excitation of the  $TM_{101}$  mode, with a source free resonance of 4.55 gigahertz. The second resonant return loss dip at 4.95 gigahertz corresponds to the loaded resonance of the  $TE_{112}$  mode, with the corresponding source free resonance as 4.93 gigahertz. And the computed 10 dB impedance bandwidth is at 21.42 percent.

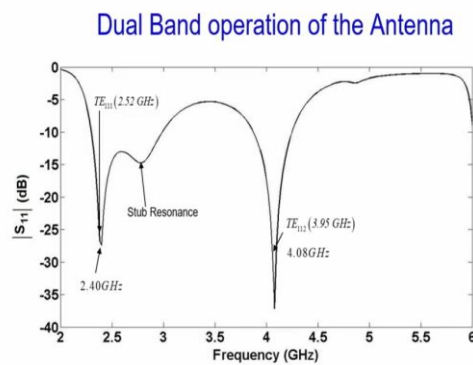
But we have to be careful that this bandwidth, which we obtain, there is a large big possibility that the radiation pattern is not going to be stable across this impedance bandwidth, which we obtained, which we report at 21.52 percent. Because on one side, we have the  $TM_{101}$  mode with a monopole like or an end fire pattern and on the other end of the bandwidth, close to the other end of the bandwidth, we have the  $TE_{112}$  mode, which has a broad side pattern.

So, the pattern is likely to change from monopole like here to broad side there, and may consist of a mixture between the two, in the bandwidth. So, therefore, the pattern characteristics will not be stable for the X offset slot. So, you see another important advantage or a deeper insight, which we obtain for the wideband structure, by using the antenna analysis, from which we get the modes, and how the modes help us to understand that this bandwidth extension may be a cause of concern.

Because if we are interested just in bandwidth extension that is fine, but if you are interested in radiation, in the radiation characteristics, in the antenna radiation performance, then we need to see that there might be and possibly would be a change in radiation characteristics because of the change in the modal type on the left side at closer to the lower resonance and the right side which is closer to the higher resonant frequencies.

Because we have the end fire mode at one side and the monopole like mode on one side and the broadside mode on the other side. So, an X offset slot, in that sense, if you are sensitive to the radiation characteristics, if it is for indoor applications, may not be a lot, we may not bother a lot, but in case we want a stable radiation characteristics, then we need to be very cautious about the X offset.

(Refer Slide Time: 20:43)



Calculated return loss of the microstrip slot coupled three-layer HDRA for dual band operation  $\epsilon_{r1}=14$ ,  $\epsilon_{r2}=1$ ,  $\epsilon_{r3}=7$ ,  $L_1=15.2\text{mm}$ ,  $L_{20}=9.45\text{mm}$ . The other parameters are the same as in Fig. 1.

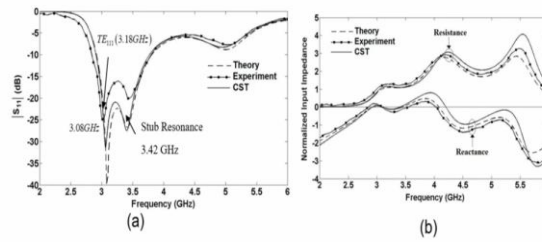


Fig. 1: Calculated, simulated and measured return loss and normalized input impedance of the microstrip slot-coupled three-layer DRA with centred slot excited in the  $TE_{111}$  mode :  $\epsilon_{r1}=9$ ,  $\epsilon_{r2}=1$ ,  $\epsilon_{r3}=4$ ,  $r_1=12.5mm$ ,  $r_2=17.5mm$ ,  $r_3=22.5mm$ ,  $L_s=14.5mm$ ,  $W_s=1.0mm$ ,  $x_w=0mm$ ,  $y_w=0mm$ ,  $\epsilon_{r2}=2.2$ ,  $h=0.508mm$ ,  $W_f=1.58mm$ ,  $L_{ob}=6.25mm$ ,  $\Delta l=0.25mm$ . (a) Return loss. (b) Normalized input impedance.

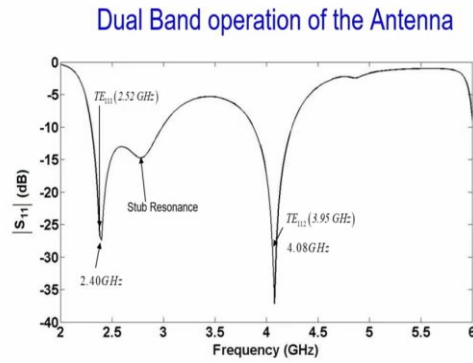
5

Now this is a dual band operation of the same DRA. The first layer permittivity 14, compared to the first layer permittivity 9 in figure 1. If you look at figure 1, it was 9;  $\epsilon_{r1}$  was 9 here. So, here we change the  $\epsilon_{r1}$  to be 14, the middle layer is 1, the third layer is at 7 permittivity. And the length of the slot is 15.2 mm and the length of the stub is 9.45 mm. So, we see that the other parameters are same as in figure 1.

(Refer Slide Time: 21:27)

- First resonance dip at 2.40 GHz is close to the source free resonant frequency of  $TE_{111}$  mode at 2.52 GHz.
- Second resonance dip at 2.76 GHz is stub resonance.
- Third resonance dip at 4.08 GHz is close to the source free resonant frequency of  $TE_{112}$  mode at 3.95 GHz.
- Calculated 10 dB impedance bandwidth of the first and second band is at 26.74 % and 9.28 %.

14



Calculated return loss of the microstrip slot coupled three-layer HDRA for dual band operation  $\epsilon_{r1}=14$ ,  $\epsilon_{r2}=1$ ,  $\epsilon_{r3}=7$ ,  $L_3=15.2\text{mm}$ ,  $L_{20}=9.45\text{mm}$ . The other parameters are the same as in Fig. 1.

13

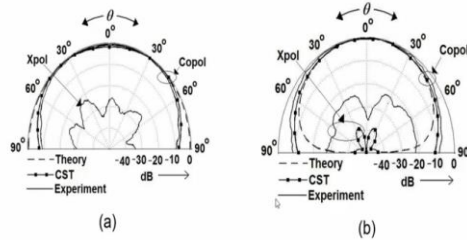
So, we see that the first resonance dip at 2.40 gigahertz is close to the source free resonance of the TE<sub>111</sub> mode at 2.52 gigahertz. So, here is the TE<sub>111</sub> mode contribution. Next the second resonance dip at 2.76 gigahertz is the stub resonance. So, this part is the stub resonance, which leads to the merger between these two modes, leads to a wider bandwidth for the first band. So, this is the first band.

And the second band which is here, if you look at that. The third resonance dip, which is contributing to the second band. So, the merger between the first and the second resonance is contributing to the first band. The second band contributed by the third resonance at 4.08 gigahertz. It is close to the source free resonance frequency of the TE<sub>112</sub> mode at 3.95 gigahertz. So, the third resonance dip at 4.08 gigahertz is close to the source free resonance frequency of the TE<sub>112</sub> at 3.95 gigahertz.

And the calculated 10 dB impedance bandwidth of the first and second band is at 26.74. This is due to the merger between the TE 111 mode and the stub resonance for the first band and 9.28 percent for the impedance bandwidth for the second band, which is contributed by the TE<sub>112</sub> mode. So, here is the first band again and here is the second band.

(Refer Slide Time: 23:09)

### Radiation Pattern of the three-layer HDRA fed by centred microstrip slot



Calculated, measured and simulated radiation patterns for centred slot at 3.36 GHz corresponding to Fig. 1. (a) x-z plane. (b) y-z plane

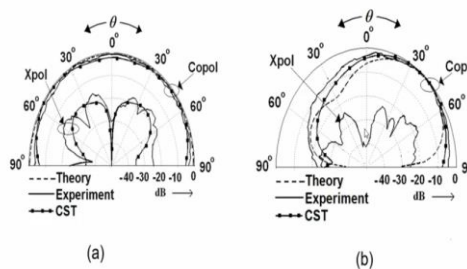


15

So, here is the radiation characteristics of the three layer hemispherical HDRA is hemispherical DRA, fed by a centered micro strip slot. So, you see the pattern characteristics are broadside, as we said, because we have excited the  $TE_{111}$  mode. So, in both the XZ plane and the YZ plane, with low cross pole.

(Refer Slide Time: 23:35)

### Radiation Pattern of the three-layer HDRA fed by y-offset slot.



Calculated, measured and simulated radiation patterns for y-offset slot at 5.5 GHz corresponding to Fig. 3. (a) x-z plane. (b) y-z plane.

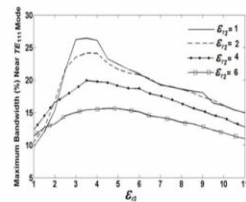


Here is the radiation pattern of the three layer DRA with the y-offset slot. So, when the slot is y offset with respect to the XZ plane. The XZ plane is symmetric with respect to the structure. So, there is no effect on the XZ plane pattern characteristics. But because the YZ plane is asymmetric with respect to the slot, it is asymmetric with respect to the slot, unlike

the XZ plane; we have the pattern asymmetry or pattern distortion in the YZ plane. Because essentially my slot is offset along the Y direction.

(Refer Slide Time: 24:24)

### Maximum Bandwidth Realization of microstrip slot coupled three-layer HDRA



(a)

The calculated Maximum optimized percentage bandwidth near  $TE_{111}$  mode of microstrip slot coupled three layer HDRA as a function of  $\epsilon_{r1}$  for different values of  $\epsilon_{r2}$ .  $r_1=12.5mm$ ,  $r_2=17.5mm$ ,  $r_3=22.5mm$ ,  $W_f=1.0mm$ ,  $x_w=0mm$ ,  $y_w=0mm$ ,  $\epsilon_{r1}=2.2$ ,  $h=0.508mm$ ,  $W_f=1.58mm$ .



17

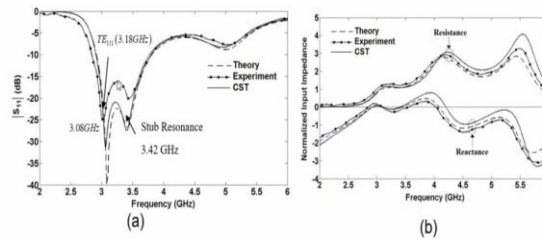


Fig. 1: Calculated, simulated and measured return loss and normalized input impedance of the microstrip slot-coupled three-layer DRA with centred slot excited in the  $TE_{111}$  mode :  $\epsilon_{r1}=9$ ,  $\epsilon_{r2}=1$ ,  $\epsilon_{r3}=4$ ,  $r_1=12.5mm$ ,  $r_2=17.5mm$ ,  $r_3=22.5mm$ ,  $L_f=14.5mm$ ,  $W_f=1.0mm$ ,  $x_w=0mm$ ,  $y_w=0mm$ ,  $\epsilon_{r1}=2.2$ ,  $h=0.508mm$ ,  $W_f=1.58mm$ ,  $L_{sub}=6.25mm$ ,  $\Delta l=0.25mm$ . (a) Return loss. (b) Normalized input impedance.



5

Next, we see the maximum bandwidth realization of the micro strip slot coupled three layer HDRA. So, here we have considered the centered slot  $X_w$  0 millimeter,  $Y_w$  0 millimeter, for the center slot case. And we see for these configurations  $r_1$  12.5 millimeter,  $r_2$  17.5 millimeter,  $r_3$  22.5 millimeter,  $W_s$ , the width of the slot 1 millimeter and the micro-strip line substrate  $\epsilon_{rs}$  2.2, the height of the micro strip substrate  $h$  0.508 millimeter and the width of the feed 1.58 millimeter. So, all other characteristics are similar to figure number 1 like  $\epsilon_{r1}$  that is 9 as in figure number 1.

So, we see that we see the maximum bandwidth versus  $\epsilon_{r3}$  with  $\epsilon_{r2}$  as a parameter. So, we see that as  $\epsilon_{r3}$  increases, we get an optimum bandwidth at  $\epsilon_{r3}$  equal to 4 and  $\epsilon_{r2}$  equal to 1.

So, this is supported by the design curves for the maximum bandwidth realization. So, this characterizes the bandwidth versus the permittivity for the three layer HDRA. Let us stop here. We will next come to the probe coupled structure and the bandwidth realization using the probe-coupled structures. Thank you.